GLASSY CARBONS

Semi-Annual Progress Report for the Period
June 1, 1971 to December 31, 1971

January 1972

ARPA Order Number: 1824
Program Code Number: 1D10
Contractor: The Regents of The University of Michigan
Effective Date of Contract: 1 June 71
Contract Expiration Date: 31 May 72
Amount of Contract: $150,263
Contract Number: DAHC15-71-C-0283
Principle Investigator: Professor Edward E. Hucke
Department of Materials & Metallurgical Engineering
The University of Michigan
Ann Arbor, Michigan 48104
(313) 764-3302

TABLE OF CONTENTS

GLASSY CARBONS

Summary

The program has three major areas of endeavor, (1) Materials Preparation, (2) Structural Characterization, and (3) Property Evaluation and Correlation.

The major accomplishment in the materials preparation program has been the successful preparation of at least some samples with cross sections up to 1.2 inches in diameter. Previous materials available have been limited to sections of about 1/8 inch, and in rare cases up to 1/4 inch. In addition, samples have been successfully made with a bulk density of from .5 grams per cm^3 to about 1.25 gm/cm^3. These materials have been prepared with a variable pore size ranging from 46 angstroms to 50 microns. These samples represent a significantly lower bulk density than previously available. Improvement in the yield of crack free material has also been made. Present efforts are toward more control over the polymerization of the furfural alcohol type resins employed together with better control over other processing variables such as heating rate.

In structural characterization, techniques have been established and results obtained on at least some samples using optical microscopy, scanning electron microscopy, transmission electron microscopy, dark field electron microscopy, wide angle electron diffraction, and wide angle X-ray diffraction.

Insufficient samples have yet been examined to draw any general conclusions, however, it has been possible to reveal various elements of structure including pores, cracks, and "crystallites" on a size scale ranging from 20 angstroms to 100 microns. In several cases changes in this structure with final heat treating temperature have been observed.

Additional structural characterization has been made by way of He density, pore size distribution (Hg porosimeter), and surface area by Knudsen flow and B.E.T. methods. Pore size has been correlated on several samples with structure obtained by microscopy. Several materials with substantial mechanical strength have been prepared having a N_2-B.E.T. surface area of around 500 m^2 per gram, a figure high enough to be of interest for chemical absorption applications.

In the area of property evaluation preliminary data has been obtained for hardness, compressive strength, tensile strength, and sonic modulus. Suitable experimental methods have been established for each measurement and data gathered on several representative samples. Too few replicate samples have been run to establish any of these properties definitively. However, on a single sample basis tensile strengths of at least 10,000 psi and compressive strengths of 50,000 psi, should be obtainable on material with a bulk density of .8 gm/cm^3. Sonic modulus has been varied over a range of $1.6 \cdot 10^6$ psi to $4.6 \cdot 10^6$ psi with further variation apparently possible.

A detailed literature study of the thermodynamic properties of carbon has shown the feasibility of determining accurately by an electrochemical cell technique the free energy and configuration entropy of glassy carbon. Preliminary measurements have been carried out, which when refined should yield directly an experimental determination of the degree of crystalline order in glassy carbon as well as more accurate thermodynamic data for the various carbon-oxygen equilibria.

GLASSY CARBONS

I. Introduction

In recent years the availability of a group of highly disordered carbons in nonparticulate form has gained the attention of materials engineers. These materials have been called vitreous or glassy carbon, due mostly to their physical resemblance to black glass. In this report they will be called glassy carbon, meaning only that they are bulk carbons possessing little if any graphitic structure. The excellent combination of properties reported leads to the belief that such materials should be capable of solving many important problems. In particular, the very low density coupled with isotropic high strength and hardness at both low and extreme temperatures, and excellent corrosion resistance have lead to many proposed applications[1]. A full exploitation of the potential applications awaits development of more detailed information on properties obtainable.

While all of the commercially available materials have rather striking simularities in reported properties there are significant variations reported in density, strength, conductivity, and stiffness, warranting the conclusion that differences in structure exist and might be further varied. All of these carbons are apparently produced by the controlled thermal decomposition of crosslinked polymers and therefore their

structures might be expected to be subject to the kind of polymer used as starting material, the evolution of the low temperature crosslinked structure, as well as the details of the higher temperature decomposition. An excellent review of the chemical steps taking place during decomposition has been published[2], but there is as yet relatively little information relating these changes to properties of the residual materials.

The commercially available materials can be obtained only after the pyrolysis is substantially complete, typically after heating to temperatures of 1000°C to 3000°C. One purpose of this study is to follow the evolution of structure from polymerization through decomposition with appropriate correlation to the properties developed.

The structural studies being carried out were chosen to yield information about structural details over a wide size range. Despite several X-ray studies[3,4] and one low temperature specific heat measurement[5] there has yet been no clear cut determination of the short range (one to ten nearest neighbors) bonding in glassy carbons. While this study will not produce an X-ray radial distribution function, it has provided controlled material for a cooperative study by neutron diffraction, where the same material is being examined by other methods. In addition, this program is endeavoring to establish the short range disorder by an electrochemical cell measurement which allows calculation of the configurational entropy of glassy carbon relative to graphite.

Atomic arrangements on the somewhat larger scale of from 20A to 1000A are being conducted with dark and bright field transmission electron microscopy as well as electron diffraction and wide angle X-ray diffraction. Other structural details on a size ranging from 100A to the macroscopic are being developed using surface replica electron microscopy and scanning electron microscopy.

From the previous studies it is apparent that the properties developed not only depend on the short range bonding of the carbon present, but on the amount, size, and distribution of the void space included in the structure. A considerable extent of void, either connected or isolated has been demonstrated at several size levels in glassy carbon materials. At the 4 to 10A level molecular sieve studies[6] have revealed an interesting structure, while small angle X-ray diffraction[7,8] surface absorption, and electron microscopy have revealed a void structure on a larger scale (20A to 1 micron). In this study small angle X-ray diffraction, scanning electron microscopy, helium pycnometry, mercury porosimetry, and surface adsorption are being selectively employed to study the pore structure.

The foregoing details should influence the mechanical properties of the resulting carbon. A representative profile of typical properties is being measured to relate to the structures produced with particular attention to be focused on obtaining as wide as possible variation in properties. For

this purpose, hardness, compressive strength, tensile strength, and modulus of elasticity have been chosen.

II. Materials Preparation

In order to have control over sample processing throughout the various stages, carbon materials have been prepared in this laboratory. Representative commercial materials are being used for comparison purposes even though they are only available after nearly complete processing.

The initial phase of the study surveyed a wide range of organic precursors and catalyst systems. At present concentration has been placed on furfural alcohol and a related commercial resin, Durez 16470*. The catalyst chosen was para-toluene sulfonic acid (PTSA). Over 90 different batches of material have been prepared yielding about 500 separate samples ranging in size from about 10 to 500 cm^3. A wide range of procedures for catalyzing the mixes, including variation of catalyst level, the initial setting time and temperature, together with variation in the subsequent pyrolysis schedule has been employed.

In many instances it was impossible to obtain samples without extensive cracking. At present an optimum procedure has not been established even though the yield of crack free samples has increased steadily. The successful survival of samples is strongly influenced by factors related to the low

---

*Hooper Chemical Company, North Tonowanda, New York.

temperature treatment of the polymer and to very uniform heating rates in the pyrolysis step. Modifications of the furnace and furnace control system have been particularly helpful in increasing the yield of good samples. Heating rates in flowing N_2 from 6 to 43°C/hr have been used up to 1000°C, with rates of about 200°C/hr employed for the range of 1000°C to 2000°C. The temperatures reported with a sample number refer to the highest processing temperature. In the low temperature range (less than 1000°C) no holding time is employed, while in the high temperature cases a holding time of 1 hour is used. At present only a limited number of samples have been produced at temperatures higher than 2000°C.

Sample cracking has in many instances been correlatable with the presence of small bubbles introduced in the mixing and casting operation. Further efforts are required to develop procedures to completely avoid this problem.

In addition, particles of an unknown origin have been found in the original Durez resin. These particles appear to cause cracking during processing and a non-uniformity in structure in the final sample. They may be clearly seen as areas about 1 micron in size in Figure 1. These particles are apparently the same as those reported by Schmitt[9]. Additional work on the occurance and elimination of these particles is planned.

Thus far it has been possible to produce sound samples of up to 1 1/8" thickness with a considerable range in structure

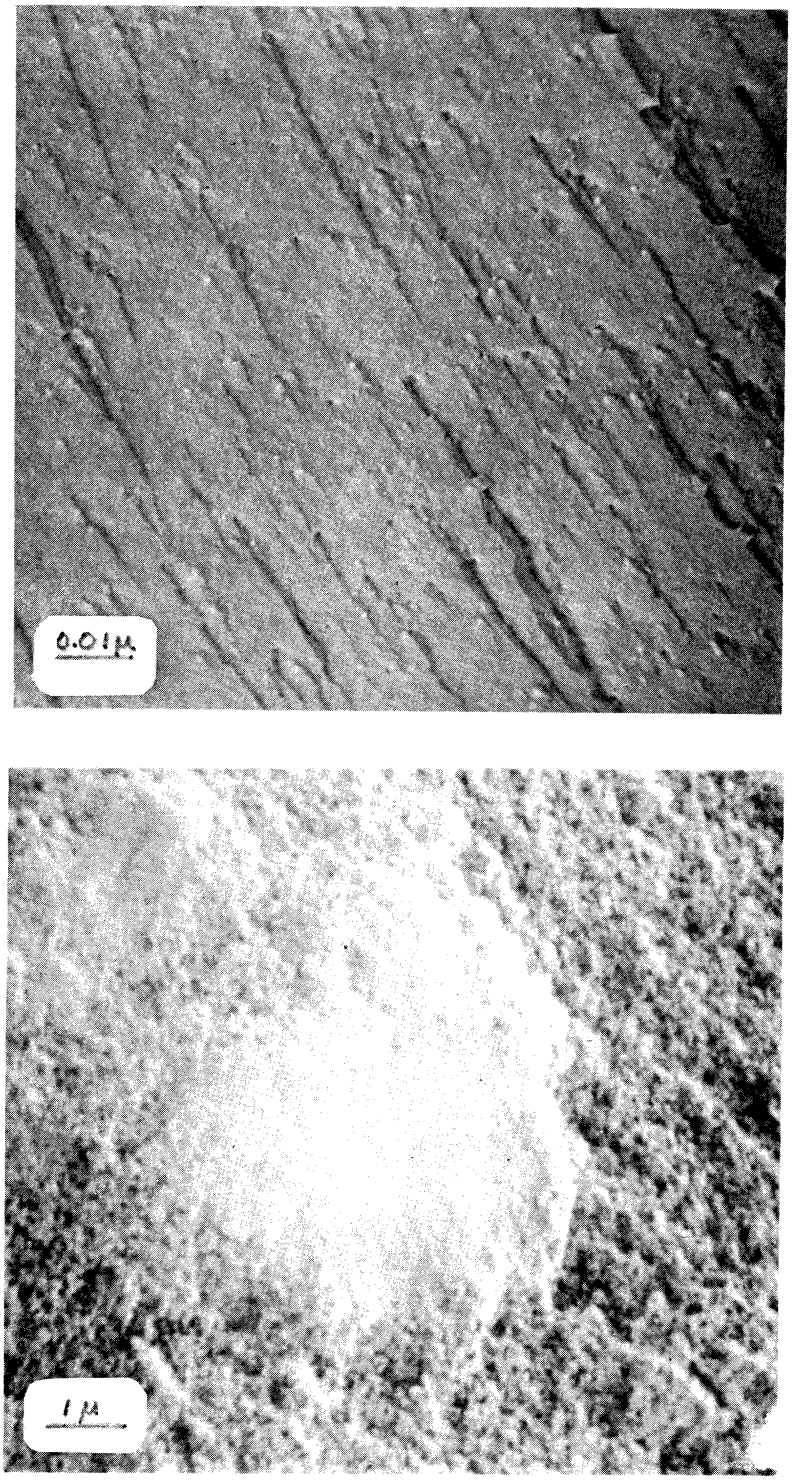

Figure 1. S.E.M. of Fracture Surface of 317-7 (700°C) showing large particles.

and densities (see later discussion). Further extension of sample size should be obtainable with more refined preparation techniques.

III. Structural Studies

While the eventual goal of this study is to correlate structure at various stages of the process with properties, the results thus far are largely drawn from samples taken at only two processing stages. The first stage corresponds to a maximum temperature exposure in the range 650-1000°C, while the second stage is that formed at about 2000°C. Further exploration of the stages of formation will proceed after appropriate techniques of sample preparation, structural analysis, and property measurement are fully developed.

The techniques chosen for structural examination fall into two broad categories with respect to the information yielded. The first yields (predominantly) information about the state of of the solid making up the structure, while the second deals mainly with the void structure. In the first category this study is employing bright field and dark field transmission electron microscopy, electron diffraction, wide angle X-ray diffraction (pinhole and diffractometer methods) and scanning and electron microscopy. The last two methods also yield information on pore structure.

Additional methods used to establish the pore structure are small angle X-ray scattering, helium pycnometry, mercury

porosimetry, and surface adsorption. An attempt is also being made to gain structural information through a precise measurement of the thermodynamics of the equilibrium

$$C_{graphite} = C_{glassy}$$

Since the effort required to carry out the above techniques varies substantially, a complete set of data will be collected on only a limited number of samples after screening with more routine tests. Apparent and real (He) density, wide angle X-ray diffraction, scanning electron microscopy (SEM), hardness, compressive strength, tensile strength, and sonic modulus are being run on representative samples of each batch in order to select appropriate samples for more intensive study. At this stage at least several samples have been examined by each of the methods mentioned, but no single sample has been examined by all.

A. Solid Structure

Microscopy and Diffraction

Intensive structural analysis has been completed on two Durez based glassy carbons, 311-19 baked at 2000°C and 311-19 baked at 750°C, the only difference being the final baking temperature. Samples for direct transmission bright and dark field electron microscopy and electron diffraction consisted of small (0.1-1.0μ diameters) particles prepared by filing clean fractured surfaces of the samples. The particles were

deposited directly on 400 mesh copper microscope grids. The edges of these particles were found to be thin enough for direct transmission of the electron beam in a JEM-6A electron microscope. In addition, two stage Pt shadowed replicas of fractured surfaces were prepared. The scanning electron micrographs were obtained from fractured surfaces that had been coated with a chromium-conductive layer. Wide angle X-ray diffraction pinhhole patterns were obtained using a 1.0mm thick sample and nickel filtered copper radiation at 35KV and 15ma for 1 hour. Diffractometer traces of the (002) and (100) peaks were obtained using the same radiation at a scan rate of 0.5°/20 min. between 2θ values of 10° and 65°.

Observation of a large number of sample particles using transmission electron microscopy revealed particle sizes ranging between 0.1 and 1.0 microns in diameter. Within each of the two samples the particles appeared to be uniform and to contain the same structural features. A typical micrograph of the sample baked at 2000°C, Figure 2a, shows the particles to be irregular in shape and to consist of irregularly shaped platelets having diameters on the order of 150-500Å. The platelets show a distinct granular texture, about 20-40Å. The platelets appear to be uniform in thickness and based on the ease of penetrability of the electron beam may be about 50-300Å thick. A typical micrograph of the sample baked at 750°C, Figure 2b, shows similar features except that the platelets and granulation were not as distinct and well defined. Platelet size is smaller, 150-350Å

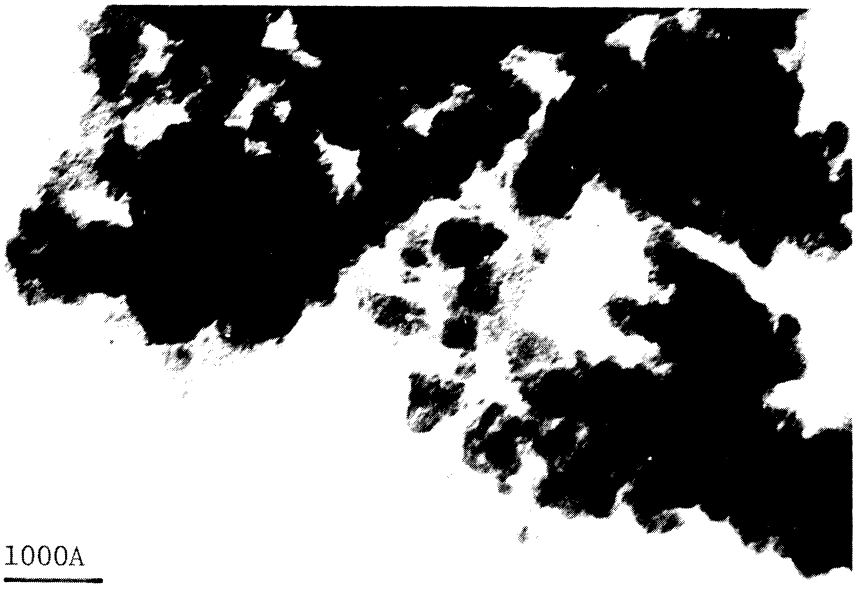

(a)

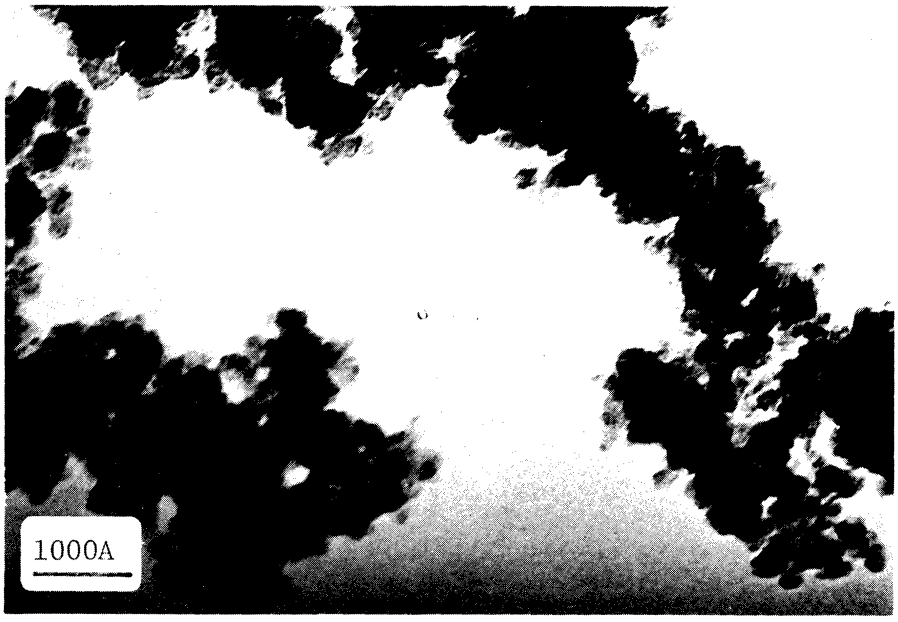

(b)

Figure 2. Bright field transmission electron micrographs of glassy carbon particles. Micrograph (a) sample 311-19, 2000°C and (b) sample 311-19, 750°C.

in diameter, while the ill-defined granulation may be 20-30Å in diameter although in some cases it is completely absent.

Electron microscopy of replicas of the brittle fractured surfaces were not as successful in revealing structural features due to the large deformation that occured in the replica when it was removed from the samples' surface. However, occasionally in the 2000°C sample large circular features, 2 microns in diameter were noticed and found to have a different type of structure. These particles are thought to be related to particles found in the original resin. Figure 3 shows the surface to be textured somewhat similar to the platelets observed in the previous micrographs. This sample has been Pt shadowed and so the smaller granulation may be due to the granulation of the Pt and not the sample.

A dark field micrograph, Figure 4, obtained from a small portion of the (002) diffraction ring show diffracting regions 20-40Å in diameter. No diffracting regions were observed when using the (100) or (110) rings.

Selected area electron diffraction patterns taken through the edges of the particles consisted of diffuse halos corresponding to the (110), (100) and (002) planes although the (002) halo was missing for the 750°C sample, probably due to sample orientation with respect to the electron beam. The d-spacings are summarized in Table 1. The diffracting halos were sharper for the 2000°C material than the 750°C material

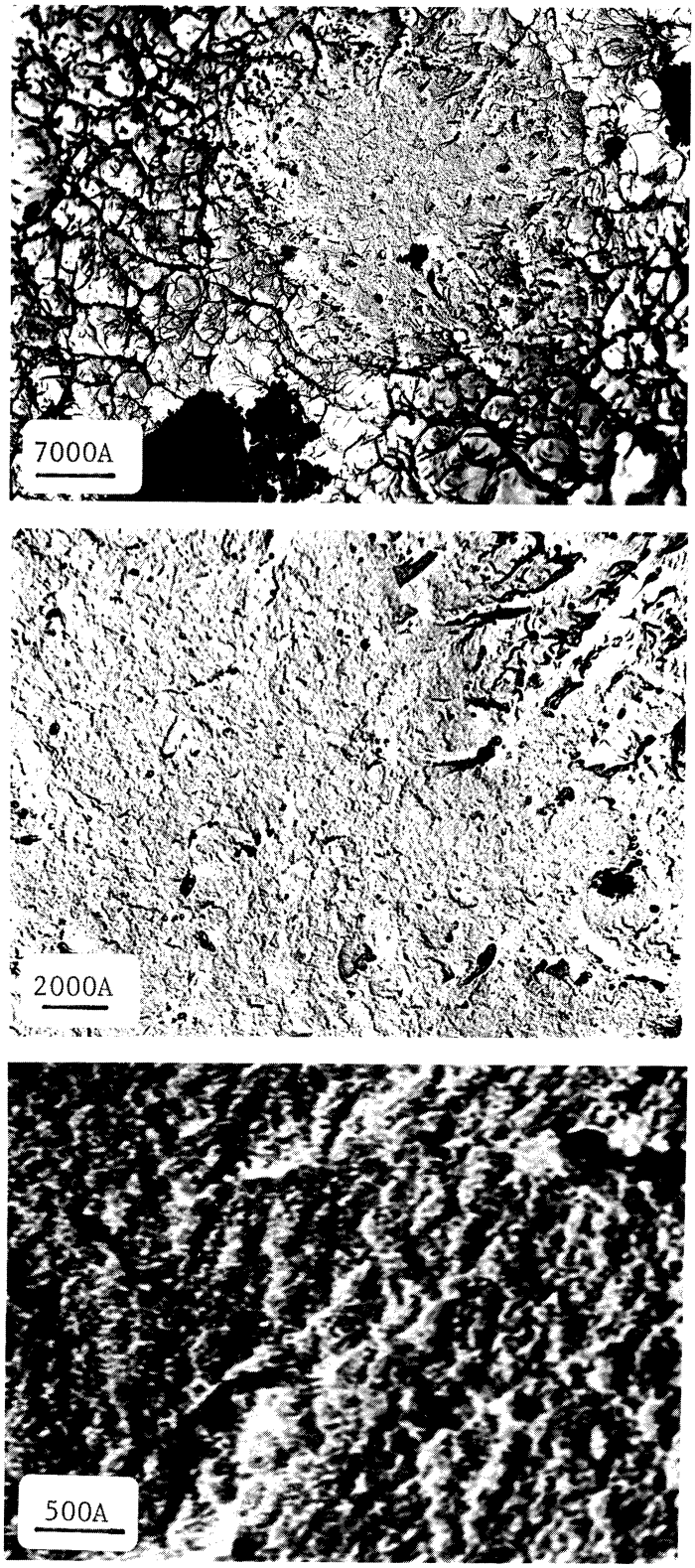

Figure 3. Bright field electron micrograph at various magnifications of two state Pt shadowed replica of a fractured surface in the 311-19, 2000°C sample.

Figure 4. Dark field electron micrograph obtained from the (002) diffraction ring. The small white dots are the diffracting regions having 20-40 Å diameters.

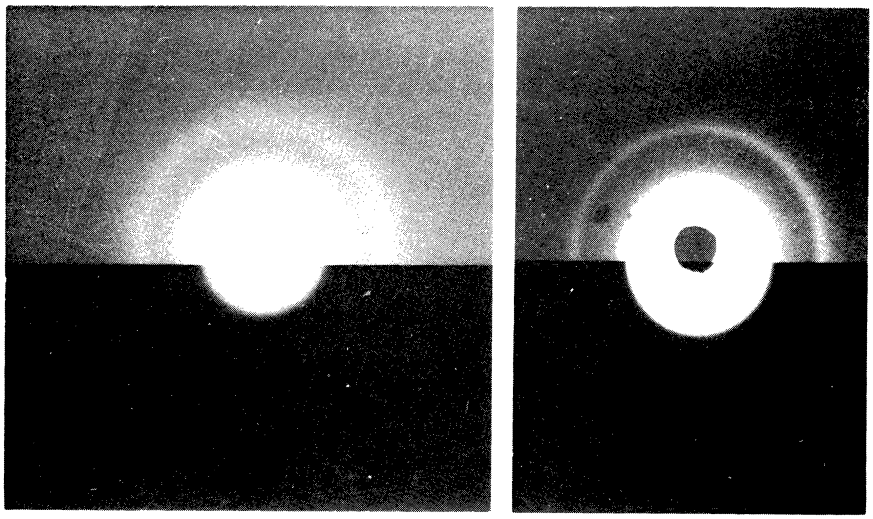

(a) (b)

Figure 5. WAXD patterns by the pinhole method. (a) 311-19, 2000°C sample, (b) 311-19, 750°C sample.

suggesting that larger or more ordered regions are present in the 2000°C material. The d-spacings and the sharpness of the diffraction pattern did not change with time in the electron beam suggesting no electron beam damage. The size of the selected area for diffraction ranged between 0.4 square microns to 1.2 square microns showing no change in the appearance of the pattern. Some variation in the sharpness of the halos was observed from particle to particle within each sample. The diffraction pattern for the one exceptional case in the 750°C material shown in Figure 6 consisted of spots instead of diffuse halos and showed more diffracting rings suggesting a more crystalline structure. Similar rather well defined diffracting regions have been occasionally encountered by Whittacre[10] in samples of glassy carbon.

Wide angle X-ray diffraction pinhole patterns, Figure 5, agree generally with the electron diffraction patterns. The 2000°C material pattern is sharper. In addition, the (002) spacings are smaller for the 2000°C material, see Table 1. Line broadening of uncorrected diffractometer traces for the 750°C material reveal a "crystalline" dimension in the c-direction of $L_c = 14.1\text{Å}$ from the (002) peak and in the a-direction of $L_a = 18.9\text{Å}$ from the (100) peak. See Table 1.

The scanning electron micrographs agree well with the transmission electron micrographs. A surface roughness of order of .1μ to 1μ is observed which is better defined in the 2000°C material. (Figures 7, 8, & 9.) The low magnification micrographs

TABLE 1

Technique		311-19,2000°C	311-19, 750°C
Bright Field E.M.			
Platelet diameter (Å)		150-500	150-350
Granulation diameter (Å)		30-40	20-30
Dark Field E.M.			
Granulation diameter (Å)		20-40	---
Scanning E.M.			
Platelet diameter (Å)		300-700	300-
X-ray Line Broadening			
(Uncorrected)	La (Å)		18.9
	Lc (Å)		14.1
	2θ of (002)		23.0°
	2θ of (100)		43.6°
	d-(002) (Å)		3.86
	d-(100) (Å)		2.08
X-ray Pinhole			
(Uncorrected)	d-(002) (Å)	3.56	3.79
	d-(100) (Å)	2.17	2.19
Electron Diffraction			
	d-(002) (Å)	3.45	None
	d-(100) (Å)	2.09	2.07
	d-(110) (Å)	1.21	1.21

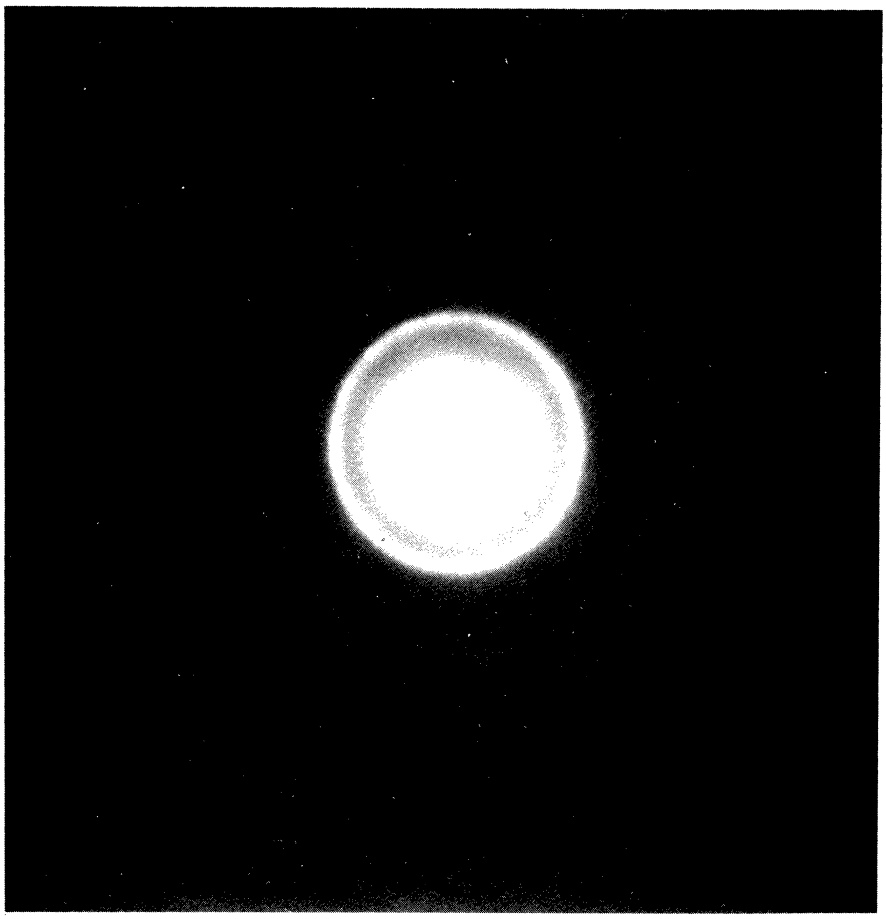

Figure 6. Electron diffraction pattern of sample 311-19, 750°C, showing spots in diffraction rings.

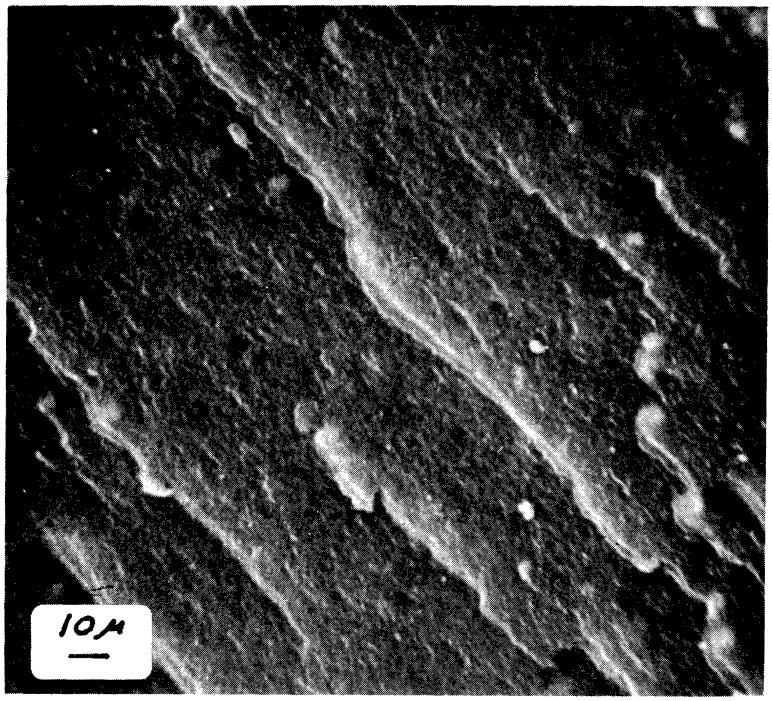

(a)

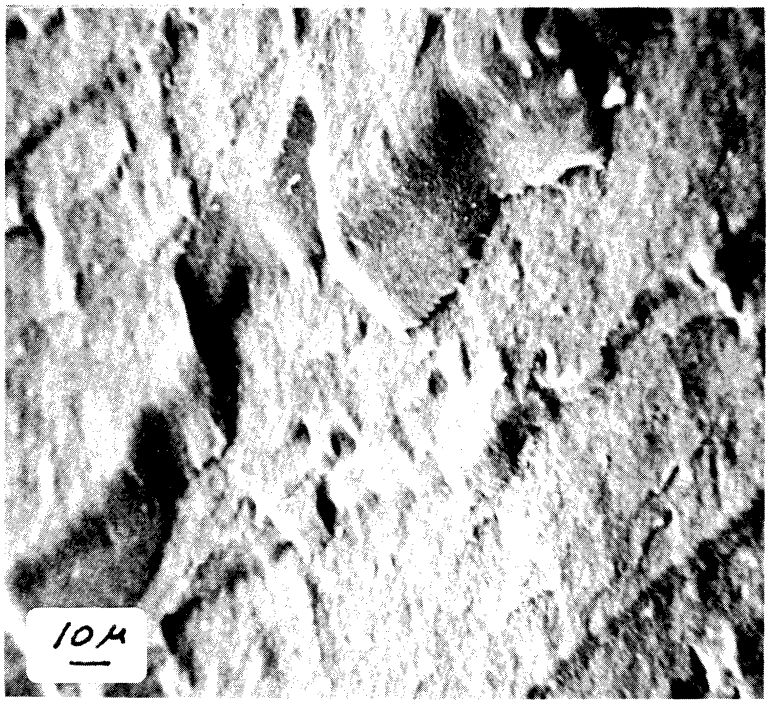

(b)

Figure 7. Scanning electron micrographs (a) 311-19, 2000°C, (b) 311-19, 750°C.

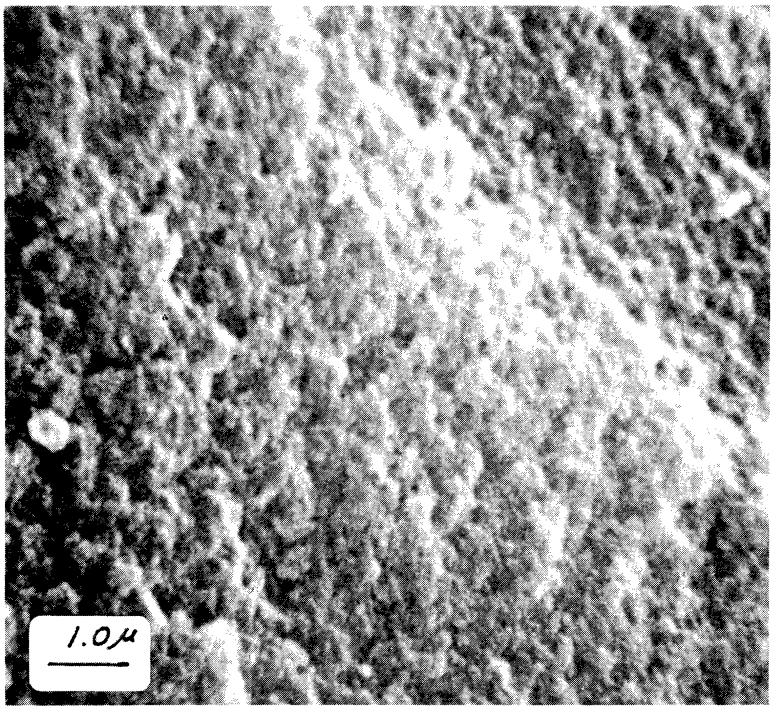

(a)

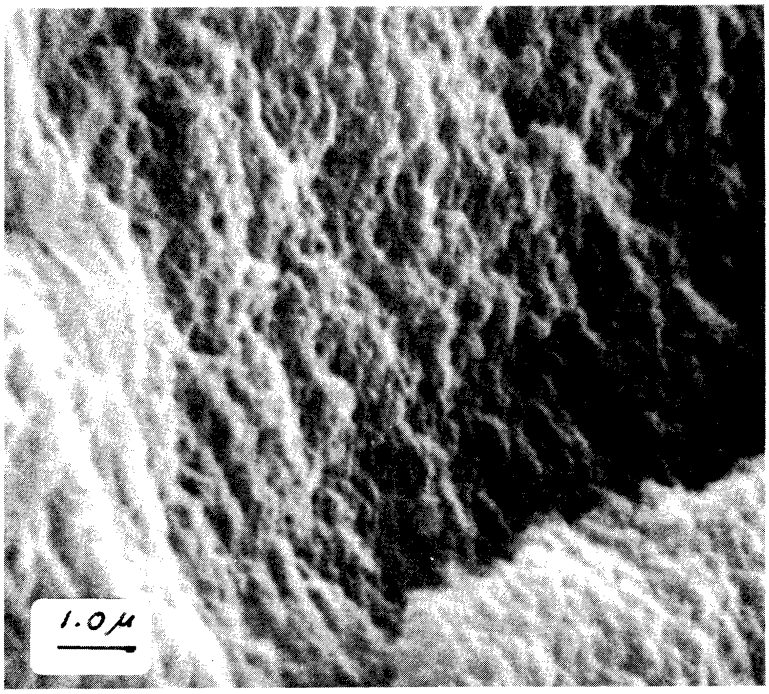

(b)

Figure 8. Scanning electron micrographs. (a) 311-19, 2000°C, (b) 311-19, 750°C.

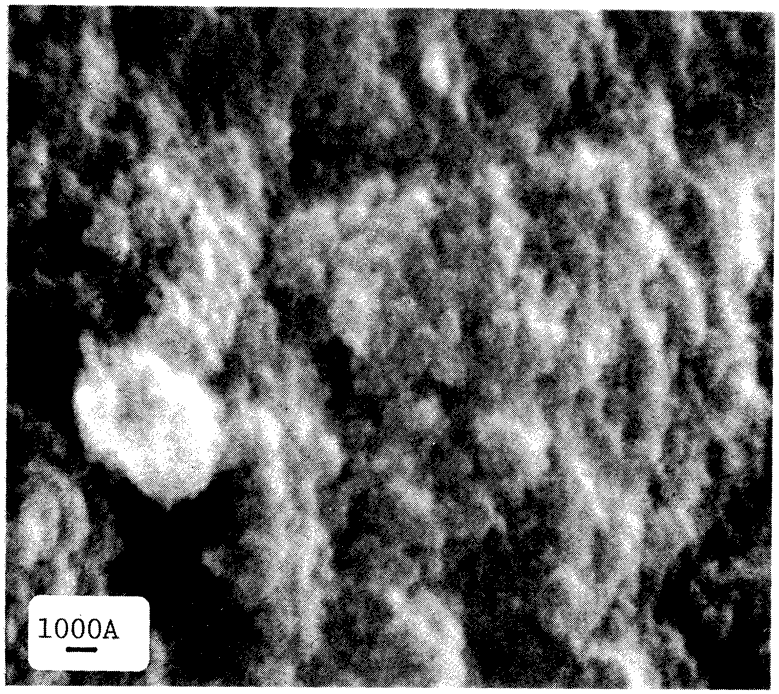

(a)

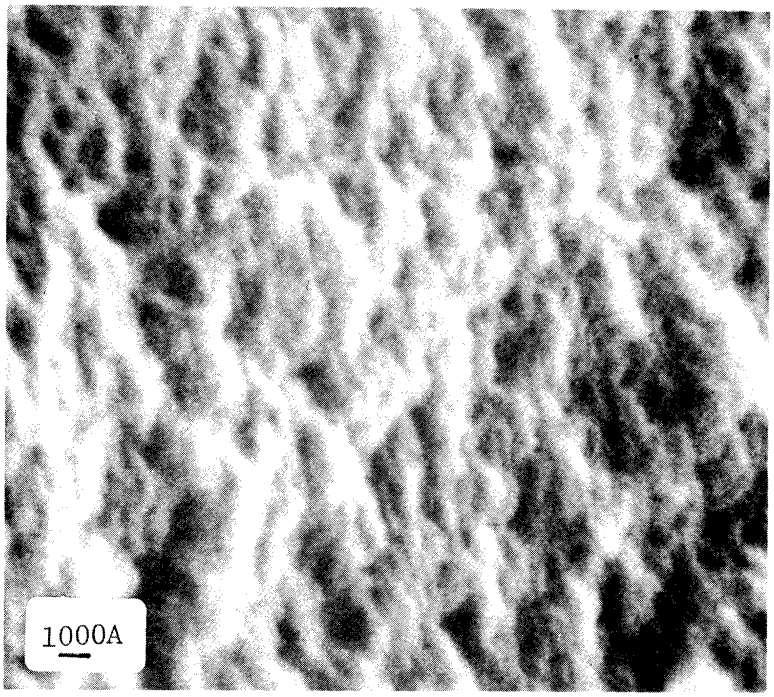

Figure 9. Scanning electron micrographs (a) 311-19, 2000°C, (b) 311-19, 750°C.

reveal a different type of fracture surface showing larger steps in the 750°C material.

The major part of both samples appears to consist of 150-500Å diameter platelets containing a 20-40Å granular microstructure. These features were sharper, as expected, for the 2000°C material than for the 750°C material suggesting a better developed, but still far from perfect structure. Electron diffraction and X-ray diffraction patterns are sharper for the higher baking temperatures supporting this observation. The granular microstructure 20-40Å in diameter was observed in both the bright and dark field micrographs possibly suggesting the materials consist of small "crystallites" of this size. This structure could be seen in the dark field studies only in the 2000°C sample. The X-ray line broadening studies yield a structural parameter which may correspond to the granular "crystallites". The interpretation of L_c and L_a strictly as "crystallite" size is, however, open to question.[11]

Although most of the material consisted of the granulated platelets occasionally other structures were observed with electron microscopy. Electron diffraction also suggests that the materials are not completely homogeneous. Further studies will be conducted to investigate these inhomogenieties.

Thermodynamics

Although there are diverse methods for gaining informati about the structure of solids on various size scales, each has its drawbacks in sensitivity, interpretation, and in ease of

measurement when applied to carbon which is not well crystallized. As a result a thermodynamic method has been proposed. The details of the feasibility of this method have been presented elsewhere[12].

The thermodynamic differences between two of the crystalline forms of carbon, i.e., graphite and diamond, are relatively well known. While less well studied, there are some data available showing differences in heat of combustion[13] and specific heat between graphites of different origins and between graphite and ill-crystallized carbons such as glassy carbon.[5,12] The heat of combustion data allows only an interpretation in terms of the average difference in binding energy between the two carbons. The temperature dependence of the low temperature specific heat can be interpreted in terms of structure, but not unambiguously.[5]

Since the reaction

$$C_{graphite} = C_{glassy}$$

involves no change in composition, the enthalpy (ΔH) and entropy (ΔS) represent a two parameter measure of the structural difference of a glassy carbon relative to graphite.

An accurate determination of the Gibbs free energy for the reaction over a range in temperature allows the separate evaluation of both ΔH and ΔS. The specific heat for crystalline graphite has been measured and at least one study of specific heat of glassy carbon has been made.[5] With the specific heat data, a separation of both the enthalpy and entropy into vi-

brational and configuration components can be made. This procedure thus yields a four parameter measure of the average difference between a given glassy carbon structure and that of graphite. The purely configurational enthalpy and entropy have a very straight-forward meaning as numerical measures of the difference in bonding energy due to disordering, and the degree of disordering respectively. Differences in the vibrational parts result from the effect of differences in average bond strength on the atomic vibrations which determine the specific heat.

In principle it is possible to calculate the configurational entropy for various simple structural models and compare for consistency with the measured value. This procedure can rule out some models, but never establish the existance of a given model. However, whatever the real structure, the data becomes a numerical measure of the disorder relative to graphite of a given carbon.

In order to be successful, the above plan must be capable of measuring ΔG as a function of temperature with high precision. Electrochemical cells using solid oxide electrolytes, as well as fused salt cells appear to offer the possibility of such a measurement.[12] These measurements should not be influenced by minor impurities and also will yield as a by-product more accurate and direct data on the equilibria

$$CO(g) + 1/2\ O_2(g) = CO_2(g) \qquad (1)$$

$$C_{graphite} + CO_2(g) = 2CO(g) \quad (2)$$

$$C_{graphite} + O_2(g) = CO_2(g) \quad (3)$$

and

$$C_{graphite} + 1/2\ O_2(g) = CO(g) \quad (4)$$

In spite of the importance of these reactions, such direct free energy measurements have not been carried out. All of the presently available thermodynamic information on carbon-oxygen equilibria is based solely on calorimetry combined with statistically calculated entropies for the gases. The accuracy of the above data depends on the ash content and crystallinity of the graphite and should be determined by direct measurement. A critical evaluation of the above factors and available data is presented as Appendix I.

At present the cell assembly shown in Figure 10 and an associated gas purification and metering train have been constructed and operated in calibration runs. The cell experiments offer excellent opportunity to check for consistency and accuracy by determinations on well characterized materials as well as independent measurements possible with different cell confiru-rations. Such calibration runs have been completed on three well known oxide systems with excellent results. The niobium-oxygen system determination is in progress. Table 2 presents the results together with Figures 11, 12 and 13. The cell employed was

$$Pt/Air(g) // Zr_{0.85}Ca_{0.15}O_{1.85} // \begin{matrix} Metal(s),\ Metal\ oxides/Pt \\ Purified\ argon \end{matrix}$$

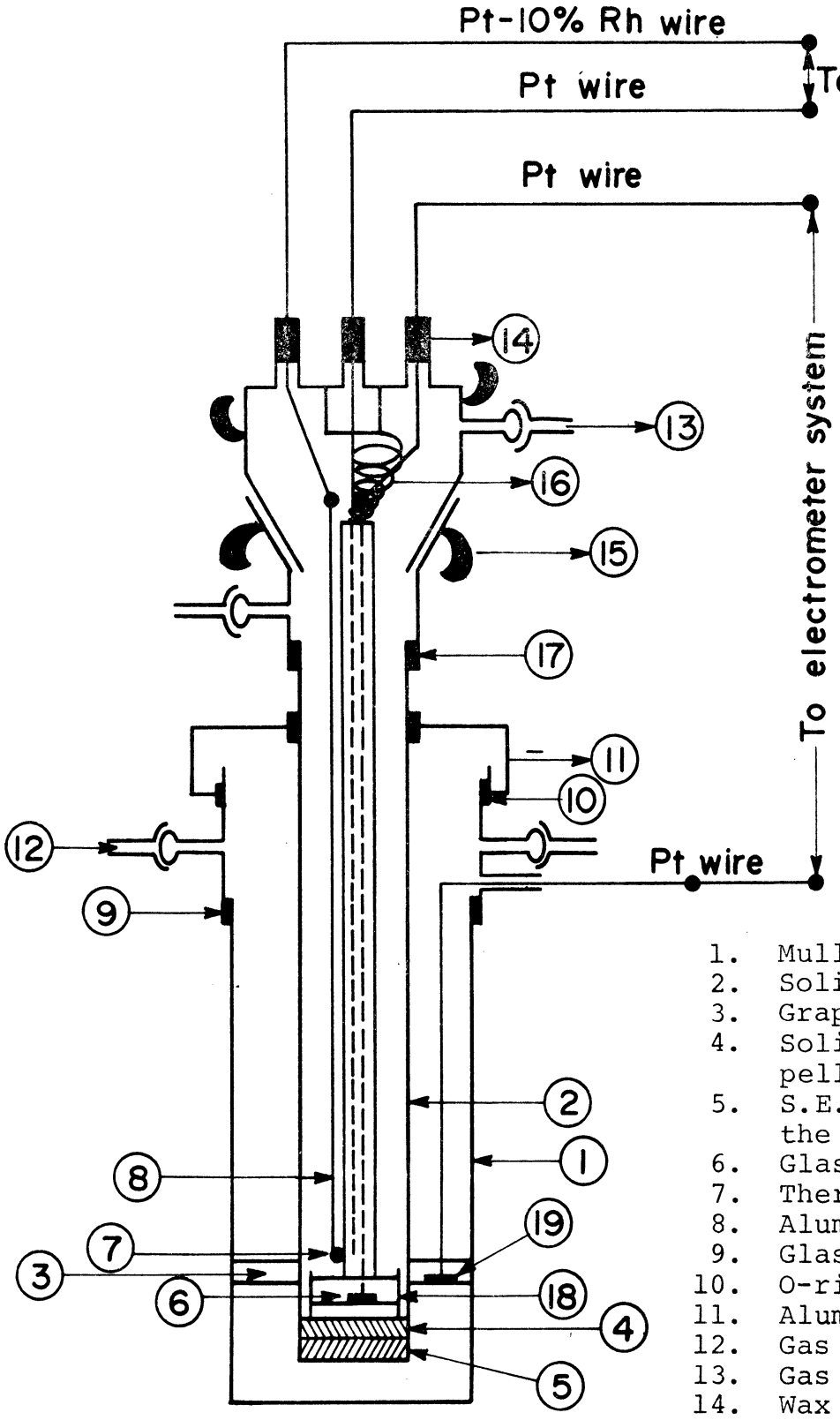

1. Mullite tube
2. Solid electrolyte tube
3. Graphite electrode
4. Solid electrolyte pellet inside the tube
5. S.E. pellet outside the tube
6. Glassy carbon electrode
7. Thermocouple bead
8. Alumina sheath
9. Glass-ceramic joint
10. O-ring
11. Aluminum coupling
12. Gas inlet
13. Gas outlet
14. Wax seal
15. Spring hook
16. Spring
17. Glass-ceramic joint
18. Vycor glass
19. Platinum ring

Figure 10.

TABLE 2

Reaction	Standard Free Energy Change $\Delta G^\circ = A + B\,T$ cal/mole, cal/mole-°K		Standard Deviation cal/mole	Correlation Coefficient
	A cal/mole	B cal/mole		
$Ni(s) + \frac{1}{2}O_2(g) = NiO(s)$	-53,988	18.9	±50	0.9999
$Co(s) + \frac{1}{2}O_2(g) = CoO(s)$	-56,665	18.0	±65	0.9997
$Fe(s) + \frac{1}{2}O_2(g) =$ "FeO"(s)	-62,646	15.1	±135	0.9987

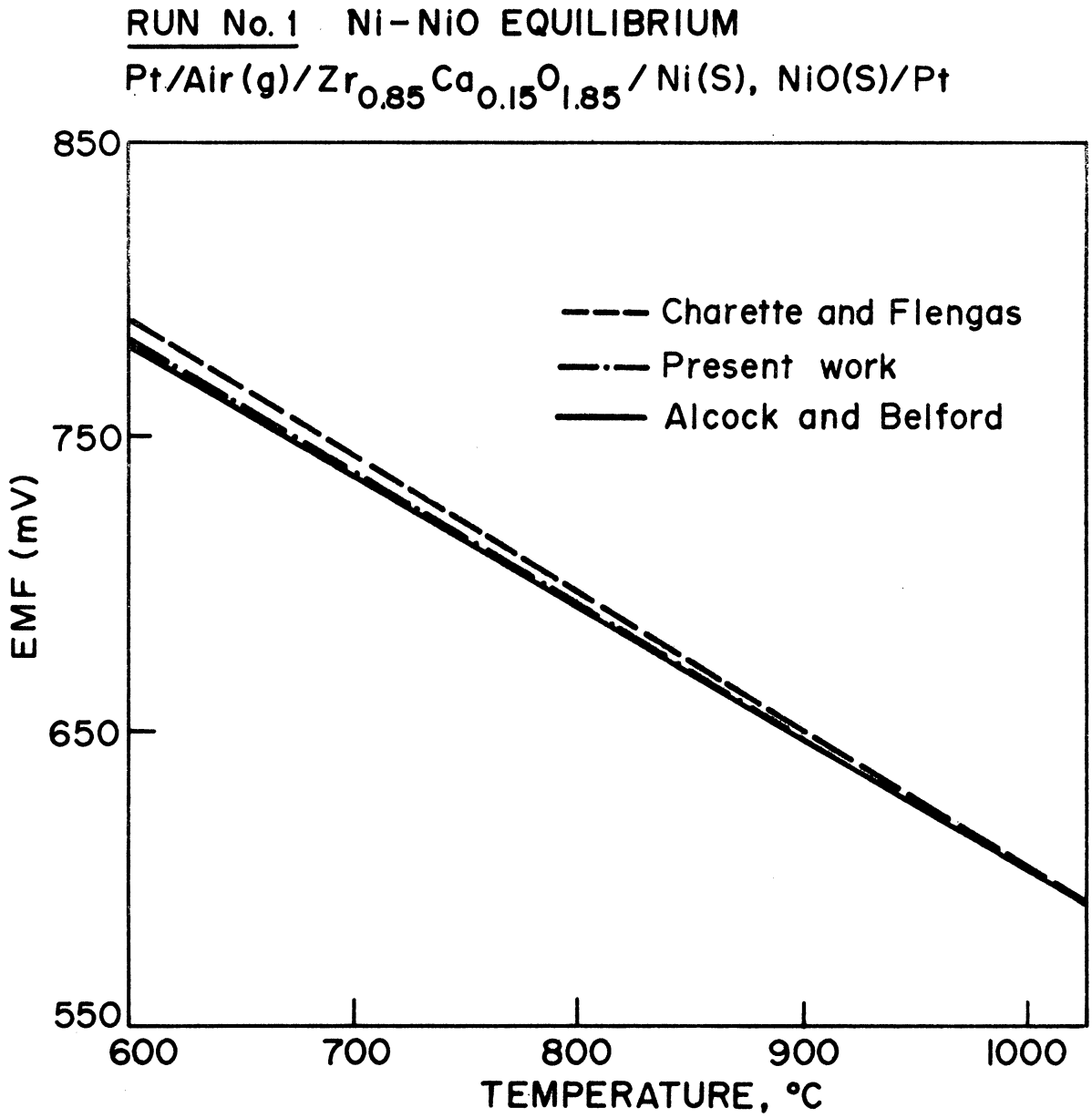
RUN No. 1 Ni-NiO EQUILIBRIUM
Pt/Air(g)/Zr0.85Ca0.15O1.85/Ni(S), NiO(S)/Pt
850
750
650
550
EMF (mV)
600
700
800
900
1000
TEMPERATURE, °C
Charette and Flengas
Present work
Alcock and Belford

Figure 11.

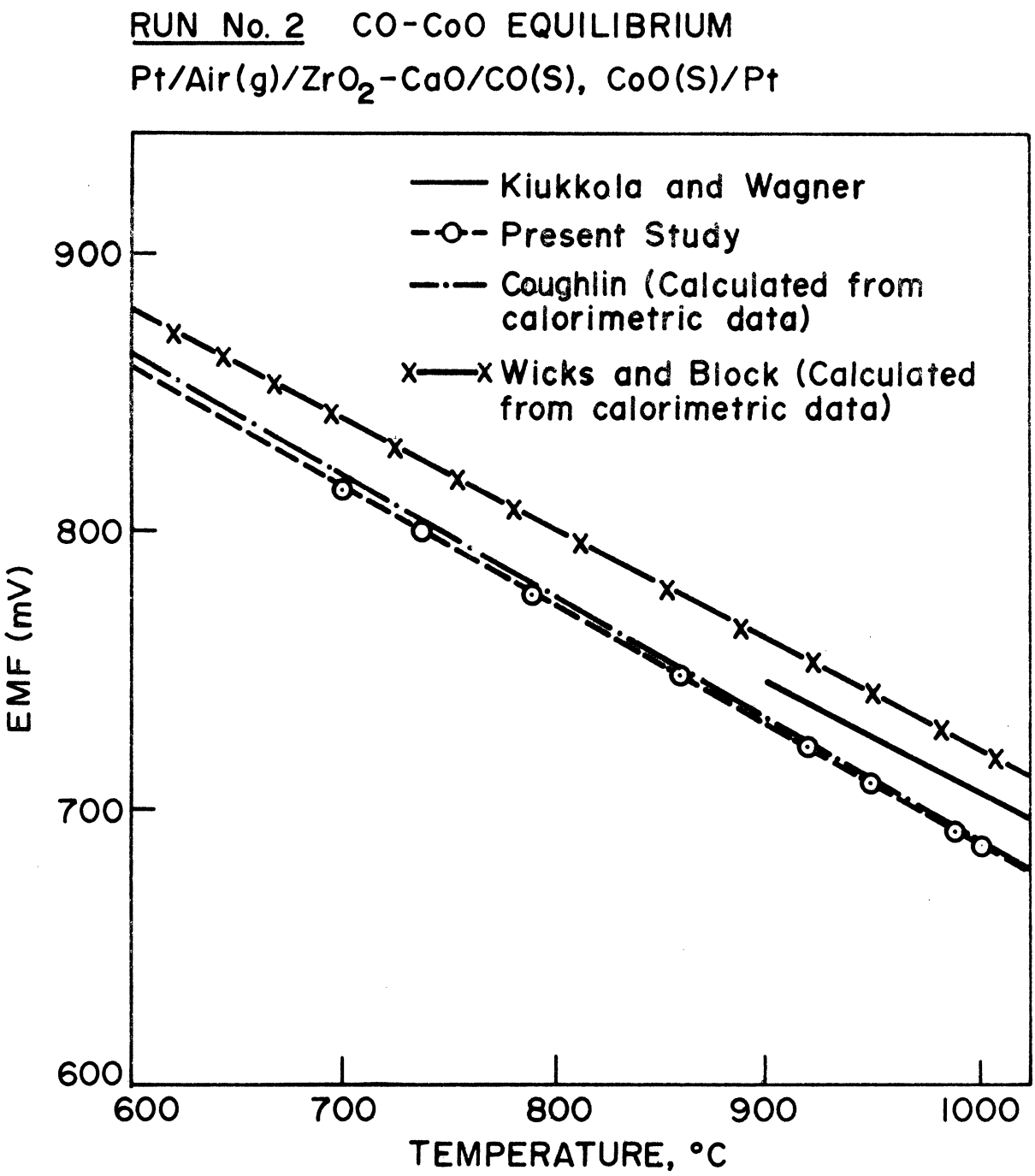
RUN No. 2 CO-CoO EQUILIBRIUM
Pt/Air(g)/ZrO2-CaO/CO(S), CoO(S)/Pt
Kiukkola and Wagner
Present Study
Coughlin (Calculated from calorimetric data)
Wicks and Block (Calculated from calorimetric data)
EMF (mV)
900
800
700
600
600
700
800
900
1000
TEMPERATURE, °C

Figure 12.

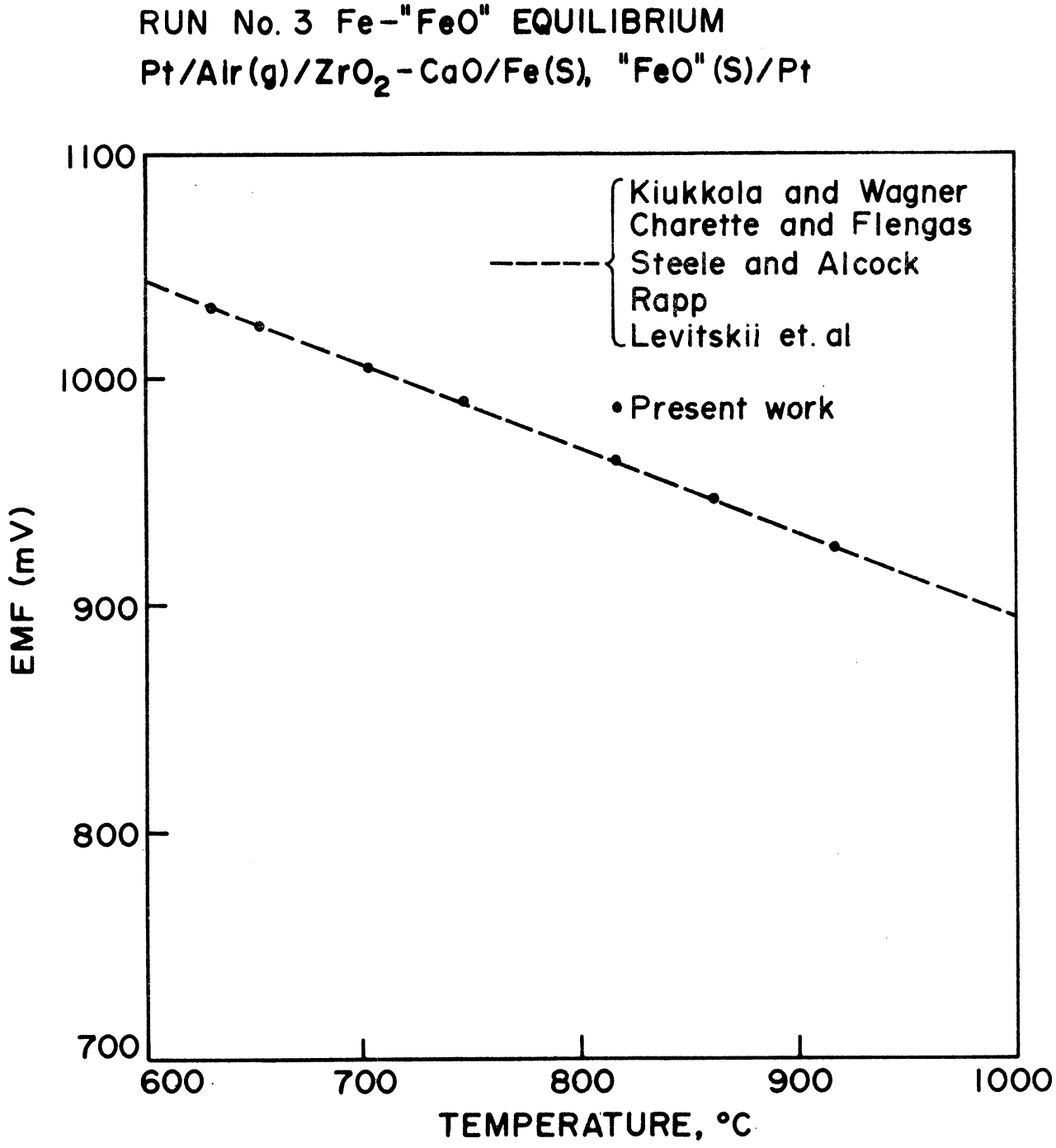
RUN No. 3 Fe-"FeO" EQUILIBRIUM
Pt/Air(g)/ZrO2-CaO/Fe(S), "FeO"(S)/Pt
Kiukkola and Wagner
Charette and Flengas
Steele and Alcock
Rapp
Levitskii et. al
• Present work
EMF (mV)
1100
1000
900
800
700
600
700
800
900
1000
TEMPERATURE, °C

Figure 13.

In addition, the first determination of the equilibrium for reaction has been made using controlled P_{CO_2}/P_{CO} in the cell,

$$Pt/Air(g)// Zr_{0.85}Ca_{0.15}O_{1.85}// CO(g), CO_2(g)/Pt$$

The data are presented in Figure 14 and are well within the scatter band of the calorimetrically determined values. Thus even these preliminary runs indicate that it will be possible to significantly narrow the scatter band which now is only about 600 cal/mole out of 47,000 cal/mole. Further refinement in technique should yield data of even higher accuracy.

In addition to the free energy data to be measured at the University of Michigan, several investigators at other laboratories have volunteered precision measurements of low temperature specific heat and heat of combustion on selected samples.

B. Pore Structure

The details of the pore structure are being investigated with a variety of techniques. Thus far no useful results have been obtained with small angle X-ray scattering due to a problem with interfacing the diffraction equipment with the counting electronics. After resolution of this problem, this technique will be employed on a limited number of samples to measure size of pore structure in the range 20-100Å where previous studies[7,8] have presented interesting results on similar materials.

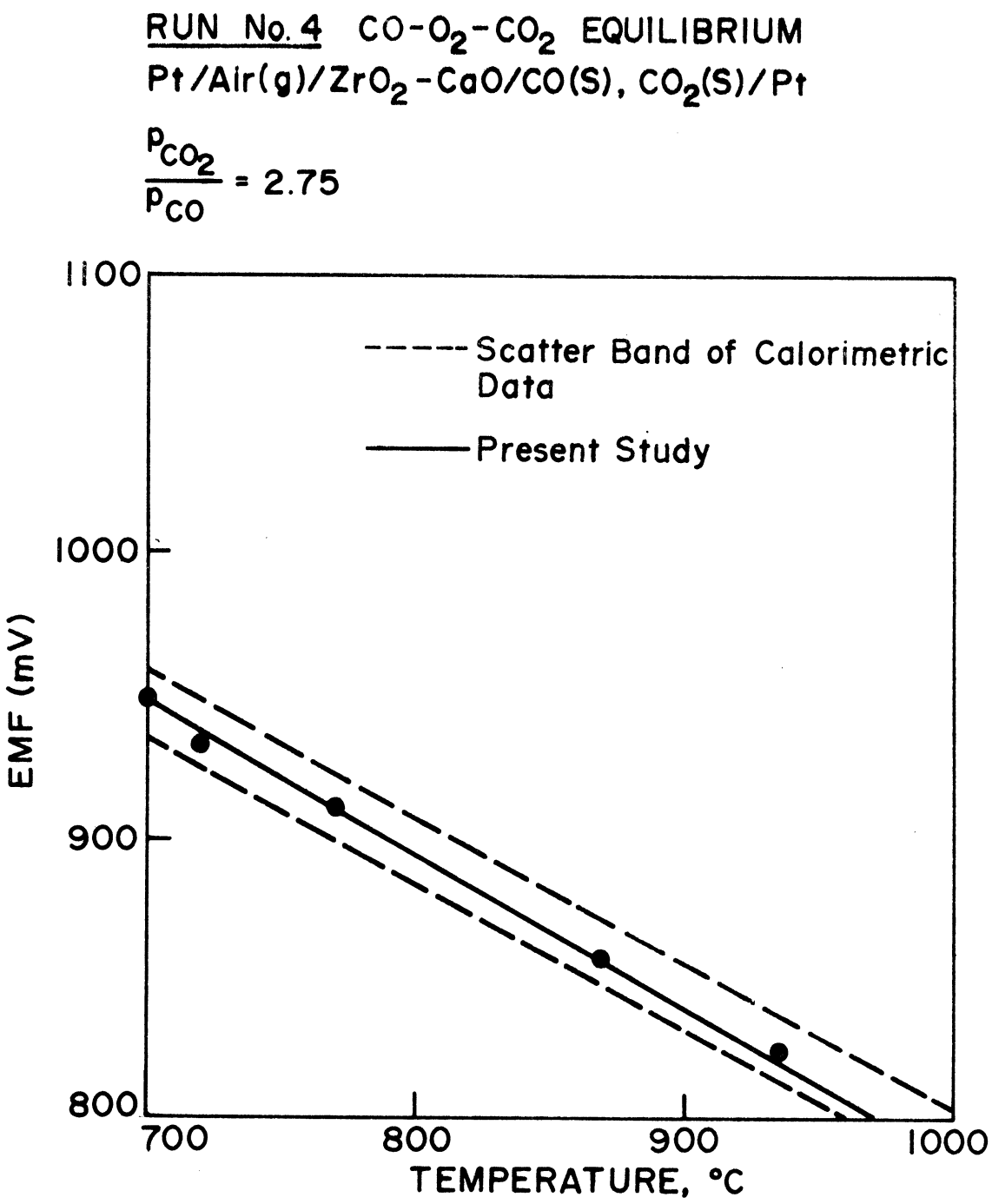
RUN No. 4 CO-O2-CO2 EQUILIBRIUM
Pt/Air(g)/ZrO2-CaO/CO(S), CO2(S)/Pt
pCO2/pCO = 2.75
1100
1000
900
800
EMF (mV)
Scatter Band of Calorimetric Data
Present Study
700
800
900
1000
TEMPERATURE, °C

Figure 14.

Helium Pycnometry

As a routine characterization of the pore volume open to He, the real density is being measured in a commercial pycnometer made by Micrometrics Inc. Corp. of Norcross, Georgia. For porous samples, data have been gathered in gross form as well as on 200 mesh powder. Thus far, samples have been produced with He densities on powdered material ranging from 1.1 gm/cm^3 to 1.8 gm/cm^3 which is a slightly wider range than has been previously reported (1.28 to 1.55 gm/cm^3)[1]. An experiment to open the closed pore structure of commercial glass carbon powder by partial oxidation (7.7 wt% loss) in air failed to yield the increased density often shown with other carbon materials. There was no significant increase in density indicating that oxidation failed to open channels between the pores. Efforts are being made to produce a still wider variation in density as well as efforts to improve the accuracy of the measurements.

In addition to real density, the apparent density of the bulk samples is determined geometrically. Samples have been produced with apparent densities ranging from about .5 gm/cm^3 to 1.2 gm/cm^3.

Surface Area

Surface area measurements have been made using three techniques. Those derived from Knudsen flow permeability and Hg porosimetry have been dropped due to lack of confidence in the results and the necessity for assuming a pore model in the latter case. While the data obtained by these methods is in

the same general range as that from B.E.T. gas adsorption, the sensitivity required to discriminate between samples appears to be inadequate.

Data on seven rather typical samples has been obtained thus far. Table 3 shows these results along with the helium densities. As expected, the lower temperature samples (700°C) showed a much higher surface area of about 500 m^2/gm compared to 20-50 m^2/gm for the 2000°C samples. This formation of an open pore structure in the low temperature range has been noted before[1] and leads to interesting possibilities for application in surface adsorption processing[6]. The values shown are about double those reported for similar carbons[1]. However, the high temperature values are also substantially higher than previously reported.

Knudsen flow derived surface area data are given where available for comparison. They are generally lower and show much less variation from sample to sample.

The density data shown were determined by the Micrometrics Instrument Corp. laboratory but also were generally in agreement with those carried out at the University of Michigan. They are higher than expected, with a definitely higher trend for the lower temperature samples. This result definitely shows the existence of a fine structure permeable to He in the low temperature samples.

TABLE 3

Sample	He Density gm/cm^3	Surface Area Knudsen Flow (m^2/gm)	Specific Surface Area (m^2/gm)
311-32, 2000°C	1.41	3.0	26.4
317-9, 700°C	1.83		506.0
319-9, 2000°C	1.70	12.5	59.9
317-12, 700°C	1.80	9.1	510.0
317-12, 2000°C	1.72		109.0
318-22, 700°C	1.79		459.0
318-22, 2000°C	1.51		49.6

Mercury Porosimetry

The mercury intrusion method of porosimetry is used for the characterization of continuous porosity[14,15]. In this investigation an Aminco* 60,000 psi mercury porosimeter is being utilized to determine cumulative pore size distribution, interconnected pore volume, density values and median pore diameter.

Typical cumulative pore volume-pore diameter curves are shown in Figure 15. These data indicate that a wide range of pore size (100A to 45μ) and pore volumes can be produced in glassy carbon materials. The curves also indicate that a rather sharp pore size distribution exists in these materials. Specific pore characteristics for several samples are indicated in Table 4. In most cases there is reasonable agreement between the real densities determined with He and Hg intrusion, indicating that at 60,000 psi almost all the pores are Hg filled. This pressure should fill an approximately 30Å pore diameter, thus supporting the finding that below 30Å the pore structure is not connected, at least in the higher temperature materials. Additional data will be gathered on lower temperature material.

Electron Scanning Microscopy

Electron scanning microscopy is employed on a fracture surface of each sample to obtain additional information on the pore structure. For the coarser materials (>200Å) the pore

*American Instrument Company, Silver Springs, Maryland.

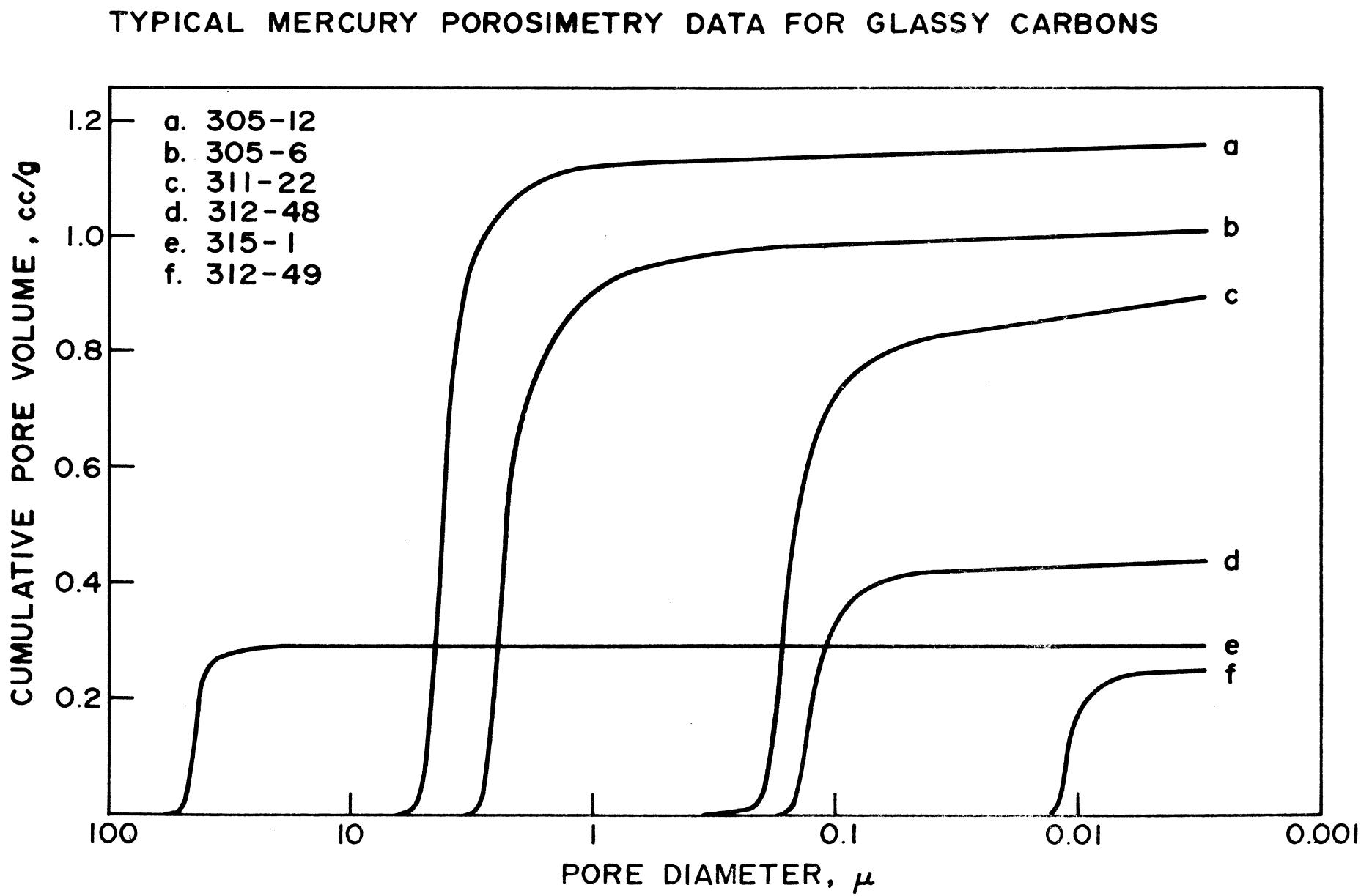
TYPICAL MERCURY POROSIMETRY DATA FOR GLASSY CARBONS
a. 305-12
b. 305-6
c. 311-22
d. 312-48
e. 315-1
f. 312-49
CUMULATIVE PORE VOLUME, cc/g
1.2
1.0
0.8
0.6
0.4
0.2
100
10
1
0.1
0.01
0.001
PORE DIAMETER, μ
a
b
c
d
e
f

Figure 15.

TABLE 4

Sample	He-ρ_{real} [1] (gm/cc)	Hg-ρ_{real} [2] (g/cc)	ρ_{app} [3] (g/cc)	MPD [4] (μ)	IPV [5] (cc/g)
305-12, 2000°C	1.55	1.562	.557	4.19	1.1560
305-6, 2000°C		1.802	.636	2.54	1.0151
311-22, 2000°C	1.00	.847	.484	.154	.8809
312-48, 2000°C	1.53	1.392	.861	.121	.4425
315-1, 2000°C	1.41	1.356	.968	45.9	.2944
312-49, 2000°C	1.34	1.404	1.031	.011	.2579
312-45, 2000°C	1.26	1.298	1.211	.0046	.0554

[1]Real density as determined by He pycnometry

[2]Real density as determined by Hg intrusion to 60,000 psi

[3]Apparent density as determined by Hg

[4]Median pore diameter from Hg porosimetry

[5]Intrusion pore volume from Hg porosimetry

structure is easily discernible with this method. However, for the finer materials, the size of the pores is equal to or finer than the 100Å resolving power of the instrument, rendering the determination of quantitative information impossible. Also the S.E.M. pictures show a surface roughness of the same order of size as the pore structure which makes pore size assessment difficult. In at least one case it has been possible to gain a good check on the Hg intrusion pore size by quantitative microscopy methods on S.E.M. pictures. Figure 16 shows the structure of one of the coarser structures which can most simply be described as a concatenation of anastomoses.

IV. Mechanical Property Evaluation

Development of testing methodology and sample preparation for characterization of the mechanical properties of glassy carbon materials is currently in progress. Mechanical properties being investigated are; hardness, compressive strength, ultimate tensile strength, and dynamic modulus of elasticity.

Hardness

Samples for hardness testing were prepared by wet grinding through 600 grit silicon carbide paper and then polishing with No. 1, 2 and 3 alumina (5, 3 and .05μ particle size) on felt wheels. A Tukon* hardness tester equipped with Diamond Pyramid (DPH) and Knoop indenters and a Tinius Olsen** Brinell

*Wilson, Mechanical Instrument Div., American Chain and Cable Company, Inc., New York, New York
**Tinium Olsen Testing Model Company, Philadelphia, Pa.

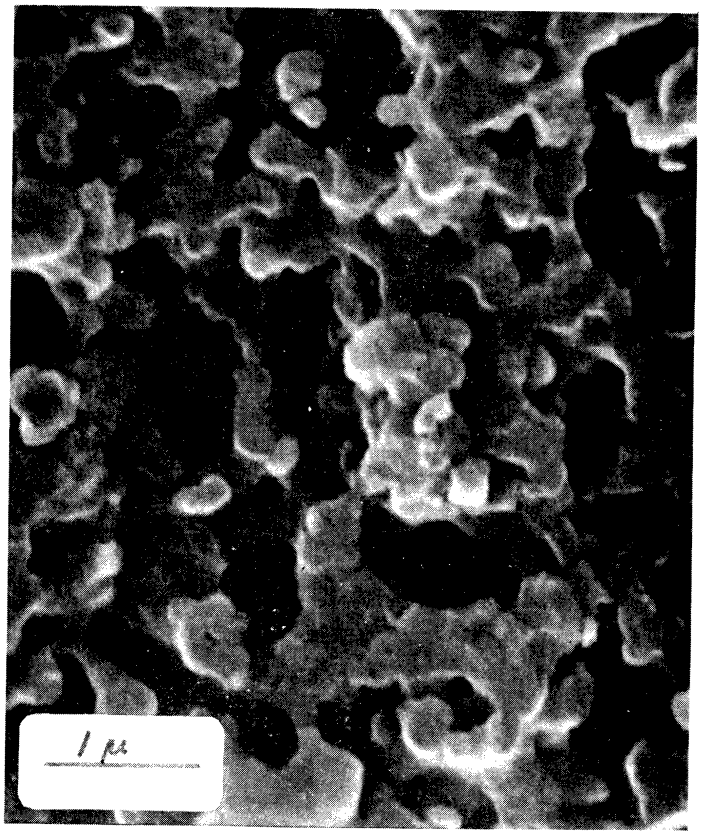

Figure 16. S.E.M. of sample 317-39 (2000°C) showing relatively coarse pore structure.

Tester equipped with a 1/16" ball were used for this work. A standard load cycle was utilized for the Tukon tester. With the Brinell tester the load was applied manually for a period of 30 seconds and then released. Loads ranging from 500 grams to 40 kilograms were used. A large variety of samples produced under various experimental processing conditions was tested. In addition, commercially available products, Atomergie V25, Atomergie V10, Beckwith D-50, Tokai 1000°C, Tokai 2000°C, and Lockheed-2000°C material were also tested.

Initially Knoop hardness determinations were made with a 500 gram load. In most cases the indentation was non-symmetrical or appeared as a line. In some cases the indentations disappeared completely after the load was released. These observations suggested that the materials studied exhibited a definite anelastic behavior. Other investigators have also observed this type of behavior.[16]

To obtain a measurable indentation with a 500 gram load it was necessary to apply a thin collodion film to the test samples prior to testing. The coating solution consisted of:

12 cc ethyl alcohol

15 cc ethyl ether

2 cc collodion

Each sample was immersed in a coating solution for 5 seconds, drained and blown dry.

Average Knoop hardness (500 gm load) values are shown in Table 5.

TABLE 5

Summary of Knoop Hardness Data

Sample Designation	KHN(500 g)
310-1, 1000°C	41
310-3, 1000°C	37
310-16, 1000°C	30
312-8A, 2000°C	42
312-13A, 2000°C	83
312-33, Heavy coating	51
312-33, Light coating	77
312-48, 665°C	27
312-48, 700°C	52
312-49, 700°C	103
312-50, 700°C	76
315-14A	69
315-46	150
317-5, 2000°C	50
317-6A, 2000°C	31
317-13, 2000°C	48
317-24, 2000°C	73
317-25, 2000°C	47
317-26*, 2000°C	19*
317-32, 2000°C	69
Atomergie V-25	140
Atomergie V-10	145
Beckwith D-50	246
Tokai, 1000°C	251
Tokai, 2000°C	186
Lockheed, 2000°C	180

*Impression disappeared - even when sample was coated by immersion for up to 1½ minutes.

No cracks or cracking sounds were observed for samples tested with the 500 gram load. Several samples were also tested with loads of 1 and 2 kilograms and exhibited no observable cracking phenomena. A few samples were measured on different models of hardness machines which have quite different loading cycles. The data from the faster loading cycle machine were higher by a value of about 10 to 20 in KHN.

Meyer hardness values were obtained for several samples using the Brinell hardness tester. Hardness values were obtained as a function of load for each sample tested. Maximum Meyer hardness values attained before the onset of cracking are shown below in Table 6.

TABLE 6

Summary of Meyer Hardness Data

Sample Designation	M_H	Load
315-46	199	17 kg*
317-24	122	7 kg
317-26	19	28 kg
Atomergie V25, 60	162	18 kg

*No cracking with loads to 36 kg.

Plots of Meyer hardness versus load exhibited much scatter and the circular indentations were difficult to measure. At some

loads only partial indentations were observed. At higher loads cracking sounds were heard and often concentric cracks were observed in the indentation.

Vickers hardness values were also measured on a group of samples as a function of load. The results are given in Table 7. Most indentations were symmetrical and easy to measure on coated samples. On one sample, 315-46, no indentations could be found on the coated sample, but could be located as an "X" shaped mark on the uncoated sample.

In general there was little variation in hardness reading with load over the range of 500 grams up to the load causing the sample to break. There was a tendency to yield a value from 10 to 20 DPH lower for loads less than 1 Kg. The DPH was consistantly higher than the KHN at 500 gm and the relative order ranking was different. In view of the weird anelastic recovery displayed, more reliable data will probably result from higher loads. However, there is reason to question all of the data available to date on glassy carbon since in no case are the values reported consistent with the scratch hardness displayed by the material. The DPH values (300 maximum) are far lower than indicated by the ability to scratch glass (Mohs' > 7).

There was a wide difference in hardness (DPH 68 to 312), but an even more pronounced difference of toughness was noted. At loads as small as 1 Kg some samples developed small cracks

TABLE 7

Summary of Vickers Hardness (DPH) Data

Sample	DPH	LOAD (Kg) FOR Cracks within Indentation	Cracks at Corners	Specimen Failure
Atomergie V25	174	3		40
Atomergie V10	171	5		40
Beckwith D-50	244	1		20
Tokai, 1000°C	233	1		20
Tokai, 2000°C	312	3		20
Lockheed, 2000°C	222	3		10
315-46, 2000°C*	240	-		No failure to 50
312-46, 680°C	100	3	5	10
312-46, 2000°C	106	3	-	20
312-45, 680°C	138	3	5	20
312-45A, 2000°C	152	3	-	10
312-33, 2000°C	68	3	3	20

*Sample uncoated.

or "scuff" marks within the impression. Several of the samples also developed cracks radiating from the indentation corners at somewhat higher loads. At still higher loads, all but one sample, 315-46, cracked apart. The load to such failure varied from 10 to over 50 Kg. This behavior is encouraging since it indicates qualitatively a range of crack toughness and that at least some carbons may fail gradually rather than catastrophically.

Thus far, the Vickers hardness test appears most suitable for routine testing of the high-density glassy carbon materials; however, additional investigation of the effects of coating, anelastic recovery of the indentation, and cracking must be undertaken. It is believed a ball test may be more suitable for testing the less dense carbon materials. A ball type hardness testing jig for adaptation to an Instron* testing machine is presently being produced. This apparatus will allow study of the anelastic relaxation also.

Compressive Strength

A series of compressive strength samples was produced by machining pieces from unbaked stock. The samples were then pyrolyzed, ultrasonically cleaned and tested. Samples 6mm in diameter and 12mm in length were tested in an Instron testing machine. In most tests, a crosshead speed of 0.05 cm/min. was used. Cushion pads, blotter paper or teflon tape, were placed

*Instron Corporation, Canton, Mass.

between the test samples and the contact blocks of the testing jig to aid in distributing the load.

Average values for compressive strength data are shown in Table 8. Compressive strength values ranged from 5,100 to 48,000 psi.

Several samples were tested at increased crosshead speeds. Of the samples tested, two materials showed an increase in strength and two exhibited no increase in compressive strength. More work is necessary to determine the effect on increased strain rate on compressive strength. Several samples were load cycled and exhibited relaxation and recovery behavior. Additional work is needed to characterize this effect.

Additional samples are being run to evaluate variables such as specimen surface finish, size, and shape.

The results shown are lower than those quoted for commercial material, however, the densities were all in the range of 1 gm/cm^3 or lower compared to about 1.55 for the commercial material. Also these data must be regarded as preliminary since specimen preparation and testing procedures are not yet optimized.

Tensile Strength

The Diametral-Compression Test[17] was used to determine the ultimate tensile strength (UTS). In this test, a right circular cylinder specimen is compressed diametrically between two flat platens. Under proper conditions induced tensile stresses cause the cylinder to fracture along the dimetral

TABLE 8

Average Compressive Strength Values of

Glassy Carbon Materials

Sample Designation	Apparent Density gm/cm^3	psi
317-5, 2000°C	.969	33,100
317-18, 2000°C	.847	5,100
317-23, 2000°C	.834	7,600
317-33, 2000°C	1.017	40,200
317-37, 2000°C	.922	40,600
317-38, 2000°C	.940	37,600
317-39, 2000°C	.889	30,700
317-40, 2000°C	.883	27,100
317-41, 2000°C	.934	10,000
317-41A, 2000°C	.898	7,400
317-41B, 2000°C	1.118	27,000
317-43, 2000°C	.895	15,000
317-44, 2000°C*	.903	33,300
317-45, 2000°C*	.866	32,300 48,300**
317-46, 2000°C*	1.027	28,200 46,400**
317-47, 2000°C	1.025	27,500

*Teflon tape cushion pad; other data blotter cushion pad.
**Head speed: 5 cm/min.

plane joining the lines of contact of the specimen and the platens.

Initially a series of samples with constant diameters and with diameter to thickness ratios of 1:1, 2:1, and 4:1 were produced and tested. Because of limited amounts of material on hand the preliminary strength data were obtained from samples having diameters of 12mm, 10mm and 6 mm, respectively.

An Instron testing machine with a crosshead speed of .05 cm/min. was used to carry out the test. Cushion pads, blotter pad or teflon tape, were positioned between the sample and contact blocks of the testing jig.

Initial trials to determine sample thickness were carried out with sample 317-37 (2000°C). Average UTS values obtained are shown in Table 9.

TABLE 9

Ultimate Tensile Strength Data for Sample 317-37(2000°C)

UTS(psi)	Size Diameter × Thickness	D/t
6,910	10mm × 2.5mm	4:1
5,140	10mm × 5.0mm	2:1
4,100	10mm × 10.0mm	1:1

On the basis of these preliminary data, samples were produced from available stock materials with a D/t ratio of 4:1. Average values of samples tested thus far are shown in Table 10.

TABLE 10

Summary of Preliminary Ultimate Tensile Strength Data

Sample Designation	Apparent Density	UTS (psi)	Diameter (mm)	Thickness (mm)
317-5, 2000°C	.969	7,500	12	3
317-18, 2000°C	.847	3,300	12	3
317-23, 2000°C	.834	1,900	12	3
317-33, 2000°C	1.017	5,600	10	2.5
317-37, 2000°C	.922	6,900	10	2.5
317-38, 2000°C	.940	4,182	10	2.5
317-39, 2000°C	.889	5,530	10	2.5
317-40, 2000°C	.883	4,500	10	2.5
317-41, 2000°C	.934	2,350	10	2.5
317-41A, 2000°C	.898	1,910	10	2.5
317-41B, 2000°C	1.118	3,900	10	2.5
317-43, 2000°C	.895	2,470	10	2.5
317-44, 2000°C	.903	5,100	6	1.5
317-45, 2000°C	.866	5,200	6	1.5
317-46, 2000°C	1.027	6,800	6	1.5
317-47, 2000°C	1.025	5,300	6	1.5

The ultimate tensile strength values varied from 1,900 to 7,500 psi. Because of the wide range of processing variables utilized in producing each type of material it is not yet possible to correlate the many variables. An additional factor which also must be determined is the effect of sample size on UTS when the diametral compression test is used. A series of samples is currently being produced which will provide information as to effect of diameter on the UTS.

The effects of pad material on strength data were also observed. Of the two different pad materials tried, the blotter paper pad (∿.5mm thick) produced the best results. Improved strengths and smoother stress-strain curves were obtained when the blotter pad was used.

On many, but not all samples, failure of the sample was not sudden in that the load dropped and then picked up again before additional "partial failures" occured. This behavior is thought to be associated with small cracks propagating prior to complete failure.

Modulus of Elasticity

Preliminary measurements of the dynamic (sonic) modulus of elasticity of several glassy carbon materials have been made with the Michigan Intermediate Frequency Electromagnetic Resonator (MIFER). This instrument can also be used for measurement of internal friction characteristics.

Preliminary dynamic modulus data are shown in Table 11. Initial measurements indicate that the dynamic modulus of

TABLE 11

Summary of Preliminary Sonic Modulus of Elasticity Data

Sample	Baking Temp. °C	Apparent Density gm/cm^3	Modulus of Elasticity
318-38	70	1.20	1.14×10^4
318-39	70	1.20	1.12×10^4
318-40	95	1.20	1.26×10^4
318-35	95	1.03	2.03×10^4
318-36	95	1.03	3.29×10^4
318-37	95	1.08	2.08×10^4
318-26	680	.915	4.62×10^6
317-48	700	.820	1.85×10^6
317-48	2000	.885	1.66×10^6

elasticity is in the range of one to four million pounds per square inch after pyrolysis. Modifications in sample geometry and refinements in instrumentation to improve the precision of the measurements are currently in progress. Quantitative internal friction data have not yet been obtained. As expected, the modulus for the precursor after setting at low temperatures is much lower, generally in the range of 10,000 to 30,000 psi. An effort will be made to follow the degree of crosslinking at low temperatures with modulus measurements. Also the modulus derived from mechanical testing will be compared to the sonic modulus.

At this time no definite conclusions about the effect of structure on mechanical properties can be drawn since structural evaluations have not yet been completed on samples where property data is available. However, it is readily apparent that by altering processing conditions such as catalization extent, baking times and temperatures, a wide range of mechanical properties can be achieved. This should allow tailoring of properties to fit specific needs when the important variables are finally sorted.

REFERENCES

1. S. Yamada, DCIC Report 68-2, Defense Ceramic Information Center (1968).

2. E. Fitzer, K. Mueller, and W. Schaefer, Chemistry and Physics of Carbon, 7, 237, Marcel Dekker, Inc., New York (1971).

3. T. Noda and M. Inagaki, Bull. Chem. Soc. Japan, 37, 1534 (1964).

4. R. W. Lindberg, Master's Thesis, Stanford University (1970).

5. Y. Takahashi and E. F. Westrum, Jr., J. Chem. Thermodynamics, 2, 847 (1970).

6. J. L. Schmitt, Jr., Thesis at Pennsylvania State University, College of Earth and Mineral Sciences Experiment Station (1970).

7. W. S. Rothwell, J. Appl. Phys., 39, 1840 (1968).

8. R. Perret and W. Ruland, Tenth Biennial Conference on Carbon, Bethlehem, Pennsylvania, 146 (1971).

9. C. R. Schmitt, AEC Research and Development Report Y-1738, Oak Ridge Y-12 Plant, Oak Ridge, Tenn. (1970).

10. Whittacre, American Ceramic Society, 24th Pacific Coast Regional Meeting, Los Angeles, California (1971).

11. S. Ergun, Tenth Biennial Conference on Carbon, Bethlehem, Pennsylvania, 164 (1971).

12. E. E. Hucke and S. K. Das, Materials Research Council Summer Study paper, (1971).

13. J. B. Lewis, R. Murdoch, A. N. Moul, Nature, 221, 1137 (1969).

14. F. A. Dullien and F. A. Batra, I & E Chem., 62, 25 (1970).

15. H. M. Rootare, Advanced Experimental Techniques in Powder Metallurgy, 5, 225, Plenum Press, New York (1970).

16. F. C. Cowlard and J. C. Lewis, J. Mat. Sci, 2, 507 (1967).

17. A. Rudnick, A. R. Hunter and F. C. Holden, Mat. Stds., 3, (1963).

18. F. C. Richardson and J. H. E. Jeffes, J. Iron and Steel Institute, 160, 261 (1948).

19. M. D. Thomson, The Total and Free Energies of Formation of the Oxides of Thirty-Two Elements, Electrochemical Soc. Inc., New York (1942).

20. O. Kubaschewski, E. L. Evans, and C. B. Alcock, Metallurgical Thermochemistry, Fourth Edition, Pergamon Press (1967).

21. R. G. Ward, An Introduction to the Physical Chemistry of Iron and Steel Making, Edward Arnold Ltd., London (1962).

22. D. R. Stull, JANAF Thermochemical Tables, Dow Chemical Co., Midland, Michigan (1965).

23. E. J. Prosen, R. S. Jessup, and F. D. Rossini, J. Res. Nat. Bur. Std., 33, 447 (1944).

24. F. D. Rossini, J. Res. Nat. Bur. Std., 22, 407 (1939).

25. D. R. Stull and H. Prophet, JANAF Thermochemical Tables,

26. K. Schwerdtfeger and E. T. Turkdogan, Techniques of Metal Research, Volume IV, Part 1, 321, Interscience Publishers (1970).

27. F. D. Rossini, D. D. Wagman, and W. H. Evans, Selected Values of Chemical Thermodynamic Properties, Nat. Bur. Std. Circular No. 500, Ser. III (1952).

28. F. D. Rossini, Selected Values of the Properties of Hydrocarbons, Nat. Bur. Std., Circular No. C461 (1947).

29. J. P. Coughlin, U.S. Bur. Mines, Bull. No. 542 (1954).

30. J. F. Elliott and M. Gleiser, Thermochemistry of Steelmaking, Addison Wesley Publ. Co., Cambridge, Mass. (1960).

31. C. E. Wicks and F. E. Block, U.S. Bur. Mines, Bull. No. 605 (1963).

32. P. Hawtin, J. B. Lewis, N. Moul, and R. H. Phillips, Phil. Trans. Roy. Soc. Ser. A, 261, 67 (1966).

APPENDIX

Critical Evaluation of the Thermodynamic Data of Carbon Oxides

In one of their classical publications, Richardson and Jeffes[18] compiled and graphically represented the standard Gibb's free energy of formation of all oxides pertinent to the iron and steel making. However, they assigned only an order of magnitude value to the accuracy of free energy data by classifying them as A (±1 Kcal), B (±3 Kcal), C (±10 Kcal), and D (>±10 Kcal). The standard free energy values of carbon oxides were taken from the compilation of Thompson[19], who had not stated the accuracy of his calculated values. Then Kubaschewski and Evans[20] and Ward[21] again compiled free energy data from the same source and quoted the same order of magnitude value of the accuracy. Therefore, all the later compilations derived from Thompson's[19] calculations give only the order of magnitude of error and their accuracy is anything less than 1 Kilocalorie, but the exact number has never been stated.

In JANAF Thermochemical Tables, first published in 1965, Stull et al.[22] compiled the thermodynamic data of carbon oxides. The $\Delta H^\circ_{f,298.15}$ value for CO_2 (Reaction 3) was taken from Prosen, et al.'s[23] paper and was corrected for the change in the molecular weight of CO_2 from 44.010 to 44.011. This correction would change Prosen et al.'s[23] value by a factor of 1.0000227. The $\Delta H^\circ_{f,298.15}$ value for CO (Reaction 4) was computed by using $\Delta H^\circ_{f,298.15}$ values of reactions 1 and 3 taken from the works of

Rossini[24] and Prosen, et al.[23], respectively. Table 12 lists the $\Delta H^\circ_{f,298.15}$ values from the original sources,[23,24] according to the present calculations, and from original and recent JANAF Thermochemical Tables.[22,25] The values of $\Delta H^\circ_{f,298.15}$ (according to the present calculations) match reasonably well with those listed in the original JANAF Thermochemical Tables,[22] but the accuracy limits attached to the values are in complete disagreement. The tabulation of Schwerdtfeger and Turkdogan[26] is based on the original JANAF Thermochemical Tables[22] and therefore they list highly exaggerated values of the uncertainty limits. However, the accuracy limits reported in recently published (June, 1971) edition of JANAF Thermochemical Tables[25] have been corrected and they match extremely well with those obtained in the present calculations.

Rossini[27] made an elaborate compilation of chemical thermodynamic properties which for carbon oxides are essentially the same as made by Rossini et al.[28] under American Petroleum Institute Research Project No. 44. Later on Coughlin[29], Elliott and Gleiser[30], Wicks and Block[31] reported the same values. They used $\Delta H^\circ_{f,298.15}$ values for reaction 1 and 3 with an accuracy of ±10 cal/mole (which, according to the present calculations, should be ±39.5, and ±10.8 cal/mole, respectively) and calculated the values of $\Delta G^\circ_{f,T}$ of reactions 3 and 4 at various temperatures. The listed accuracy of $\Delta G^\circ_{f,298.15}$ values of reactions 3 and 4 are 30 and 20 cal/mole, respectively. Using equation 5, and the most accurate values of $\Delta S^\circ_{f,298.15}$

TABLE 12: Critical Evaluation of Thermodynamic Data of Carbon Oxides

Reaction	$\Delta H^\circ_{f,298.15}$ cal/mole		$\Delta G^\circ_{f,298.15}$ cal/mole		$\Delta G^\circ_{f,1000}$ cal/mole
	Source	Value	Source	Value	Present Calculation
$C(gr.)+O_2(g)=CO_2(g)$	[23]	-94,051.8±10.8	*	-94,260.6±55.8	-94,628.6±100.8
	*	-94,053.9±10.8	[29]	-94,260.0±30.0	
	[22]	-94,054.0±30.0	[22]	-94,265.2	
	[25]	-94,054.0±11.0	[25]	-94,265.2	
$CO(g)+\frac{1}{2}O_2(g)=CO_2(g)$	[24]	-67,636.1±28.7	*	-61,480.8±73.7	-46,769.6±118.7
	*	-67,637.6±28.7			
	[22]	-67,636.5			
	[25]	-67,638.0±30.0			
$C(gr.)+\frac{1}{2}O_2(g)=CO(g)$	[24]	-26,393.8±30.8	*	-32,779.8±130	-47,859.0±219.5
	*	-26,416.3±39.5	[29]	-32,808.0±20.0	
	[22]	-26,416.5±620	[22]	-32,786.0	
	[25]	-26,417.0±40.0	[25]	-32,786.0	
$C(gr.)+CO_2(g)=2CO(g)$	[24]	41,242.3±58.4	*	28,701.0±203	-1,089.4±338.2
	*	41,221.3±68.2			

*Present Calculation

of reactions 1 and 3 (-20.650 ± 0.045 and 0.693 ± 0.045 cal/mole-°K, respectively) the calculated accuracy of $\Delta G°_{f,298.15}$ values of reactions 3 and 4 are ±55.8 and ±129.5 cal/mole, respectively. The accuracy of $\Delta S°_{f,T}$ used in the present calculations incorporates errors in the experimental heat capacity values as well as their numerical integration. Error in $(\Delta H°_{f,T} - \Delta H°_{f,298.15})$ values are taken to be T times error in $\Delta S°_{f,T}$ values.

$$\delta\left(\Delta G°_{f,T}\right) = \delta\left(\Delta H°_{f,298.15}\right) + \delta\left(\int_{298.15}^{T} \Delta C_p \, dT\right) + T\delta\left(\Delta S°_{f,T}\right) \quad (5)$$

Table 12 shows $\Delta G°_{f,T}$ values of reactions 1-4 at 298.15 and 1000°K as obtained in the present calculations, listed by Coughlin[29], and original and recent JANAF Thermochemical Tables.[22,25]

The thermochemical calculations and the extended discussion of their probable accuracy depend heavily on accuracy of the heat of combustion of graphite (reaction 3) as reported by Prosen et al.[23] in 1944. When an accuracy of ±10.8 cal/mole has been reported, one has to critically consider the effects of impurity content, impurity composition, pretreatment, and the kind of graphite. Experimentally it is almost impossible to determine the weight of ash present in the sample after combustion, and in calculating the results it is necessary to assume that any residue present in the crucible after combustion has the same composition as in the original graphite. This method of correcting for the weight of ash is not necessarily sound because the assumption is made that the impurities are

originally present in the graphite in the same form as they are found in the ash, namely, as oxides.[32] It is more correct to assume that the impurities are present as carbides which oxidize during the combustion process. Thus, not only will the weight of ash differ from the original impurity content, but in addition, a significant quantity of heat will also be evolved by the oxidation of carbides. The effect of the impurity content on the heat liberated per gram of graphite burned can be demonstrated by considering the behavior of a graphite which has an ash content of 300 ppm; that is 1 gram of graphite produces 0.3 mg of ash. During the thermal pretreatment silicon and calcium present in the graphite are converted into carbides which in turn, during the combustion, undergo exothermic reactions:

(i) $SiC + 2O_2 = SiO_2 + CO_2$ ($-\Delta H°_f$ = 269.1 Kcal/mole or 9578 cal/g Si);

(ii) $CaC_2 + 5/2O_2 = CaO + 2CO_2$ ($-\Delta H°_f$ = 325.0 Kcal/mole or 8109 cal/g Ca).

If the concentrations of silicon and calcium impurities are both x mg/g carbon, then on combustion by stoichiometry, 2.14x mg of silica and 1.40x mg of calcium oxide will be produced for every gram of carbon. The weight of ash will be 3.54x mg. Equating this with the assumed figure of 0.3 mg gives x as 0.085. Thus the silicon and calcium content of the original graphite is 0.085 mg/g and consequently the SiC and CaC_2 contents are 0.121 and 0.136 mg/g, respectively. The amount of carbon which burns as graphite is depleted by the amounts combined as carbides and

these are 0.036 mg/g as SiC and 0.051 mg/g as CaC_2, leaving 0.999743 g/g of "free" carbon. The heat of combustion value (94,051.8 cal/mole) reported by Prosen et al.[23] can be written as:

heat of combustion/g ash free graphite

$$= \frac{\text{observed heat release/g sample}}{1 - \text{ash content/g sample}}$$

Thus, the observed heat release = 7830.47(1-0.0003) = 7828.12 cal/g. Therefore, 0.121 mg of SiC and 0.136 mg of CaC_2 would liberate 0.6g and 0.81 cal, respectively, and the heat liberated by the combustion of 0.999743 grm of "free" carbon in graphite is 7826.62 cal. This yields a value of 7828.63 cal/grm or 94029.7 cal/mole for the true heat of combustion of graphite. It can be seen that the apparent heat of combustion measured by Prosen et al.[23] is 22.1 cal/mole (94,051.8 - 94029.7) higher than the true value for a graphite assumed to contain equal Si and Ca impurity and totaling 300 ppm of ash.

If the graphite sample was not prepared by heating to at least 2700°C in an inert atmosphere, the heat of combustion obtained was significantly higher (40 cals/mole).[32] This result which was fully corrected for ash characteristics, shows the significant effect on heat of combustion due to difference in degree of graphitization. However, the value of heat combustion reported by Prosen et al.[23] is an average of 17 measurements on Buckingham natural graphite and various artificial samples, with varying degrees of graphitization and ash characterisitcs.